Open Access

Research Article

PRNANO

Precis. Nanomed. 2025, 8(1):1406-1413

ANDOVER HOUSE

Paranoid Schizophrenia Diagnosis via Complex Network Analysis on EEG Data

Miguel Angel Vargas Cruz*

Grupo Alianza Empresarial, Montecito 38 Piso 25 Oficina 15, Colonia Nápoles CP 03810, Ciudad de México.

Submitted: December 7, 2024 Accepted: January 17, 2025 Published: January 21, 2025

Graphical Abstract

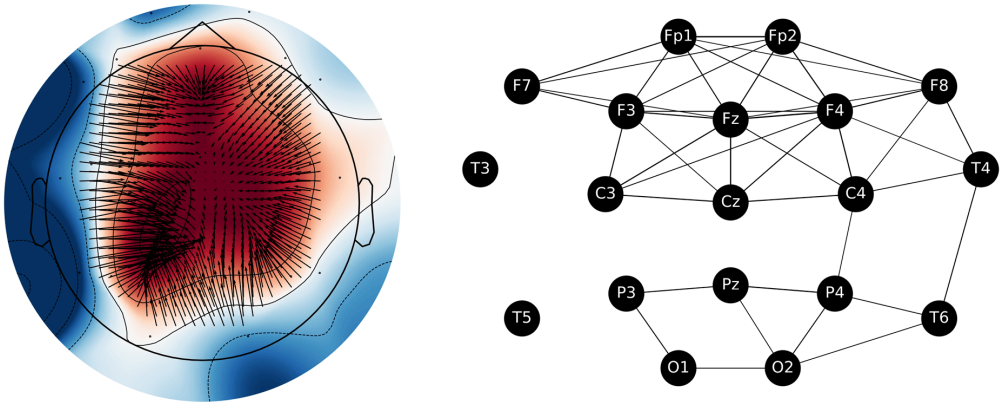

Abstract

Accurate and efficient diagnosis of schizophrenia remains a critical challenge in clinical neuroscience. This study presents a novel approach leveraging complex network analysis and Discrete Fourier Transform (DFT) applied to electroencephalogram (EEG) data for diagnosing schizophrenia. Due to its high versatility and low cost, EEG offers significant potential for widespread clinical application. Utilizing a rigorously validated dataset comprising 28 subjects—14 diagnosed with paranoid schizophrenia and 14 healthy controls—, we achieved a classification accuracy of 93%. The methodology emphasizes computational efficiency, scalability, and flexibility, making it a promising tool for clinical applications. The findings demonstrate the potential of integrating advanced signal processing techniques with machine learning algorithms to advance psychiatric diagnostics.

Keywords: Schizophrenia, Diagnosis, EEG, Complex Networks, Discrete Fourier Transform, Machine Learning, Classification Accuracy, Computational Efficiency, Random Forest, GridSearchCV

Purpose, Rationale, and Limitations

The primary objective of this study is to develop a computationally efficient, scalable, and flexible diagnostic tool for schizophrenia using electroencephalogram (EEG) data. By integrating complex network analysis with a Discrete Fourier Transform (DFT), the research aims to achieve high classification accuracy while maintaining low computational costs, facilitate widespread clinical application, and enable real-time diagnostic processes.

Schizophrenia is a debilitating mental disorder that significantly impacts individuals' cognitive and emotional functioning. Early and accurate diagnosis is paramount for effective treatment and management. Traditional diagnostic methods rely heavily on clinical interviews and subjective assessments, which can

* Correspondence: miguelangel@grupoalianzaempresarial.com

lead to delays and inconsistencies. EEG-based diagnostics offer an objective alternative. This study addresses these challenges by introducing a novel methodology that combines complex network analysis with DFT, aiming to enhance diagnostic accuracy while ensuring computational feasibility.

This study is constrained by a relatively small sample size of 28 subjects, comprising 14 individuals diagnosed with paranoid schizophrenia and 14 healthy controls. The limited diversity within the sample may affect the generalizability of the findings. Additionally, the dataset's homogeneity may not capture the full spectrum of schizophrenia manifestations, limiting the model's applicability across varied populations. Future research should involve larger and more diverse cohorts to validate and extend the current findings.

Introduction

The study aims to replicate a previously reported method[17] that claimed 100% classification accuracy. The primary objective is to investigate causality rather than the method itself. However, because the original code was unavailable, the replication (the code is in the Appendix) resulted in a lower accuracy of 67%, highlighting the critical need for reproducible research practices in the field.

Experimental Design

The study employs a cross-sectional design utilizing EEG data from 28 subjects. The experimental workflow encompasses data acquisition, preprocessing, feature extraction through complex network analysis and Discrete Fourier Transform (DFT), and classification using a Random Forest algorithm optimized via GridSearchCV within a Stratified 14-fold Cross-Validation framework. Stratified K-fold cross-validation ensures a balanced representation of classes in each fold, mitigating potential biases due to class imbalance.

Hypothesis

The integration of complex network analysis and DFT applied to EEG data can accurately distinguish between individuals with paranoid schizophrenia and healthy controls, achieving high classification accuracy with minimal computational resources.

Methods

Data acquisition

EEG data were sourced from the dataset provided by Graph-based analysis of brain connectivity in schizophrenia[1]. The dataset consists of recordings from 28 subjects: 14 diagnosed with paranoid schizophrenia and 14 healthy controls. The EEG data were preprocessed to isolate specific channels relevant to brain connectivity analysis.

These topographic maps and graphs reveal substantial variability in brain activity across subjects, complicating the identification of consistent patterns. This variability prompted the exploration of multiple approaches to enhance classification accuracy.

The development of this methodology was significantly supported by the T5 channel, which played a crucial role in refining the process. The insights from its implementation provided key guidance in enhancing the classification framework and optimizing the procedure. The final version pick O1, O2, P4, T5, Pz and T6 channels.

Preprocessing

EEG signals were standardized using the StandardScaler to ensure uniform scaling across channels. Adjacency matrices representing brain connectivity were generated by computing Pearson correlation coefficients between selected EEG channels over specified time windows. Specifically, six channels—O1, O2, P4, T5, Pz, and T6—were selected based on their relevance to brain connectivity patterns implicated in schizophrenia.

Schizophrenia:

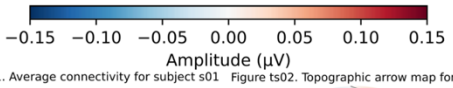

Figure ts01. Topographic arrow map for s01

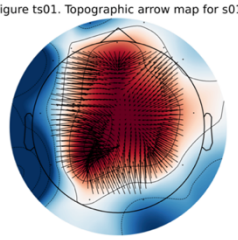

Figure gs01. Average connectivity for subject s01

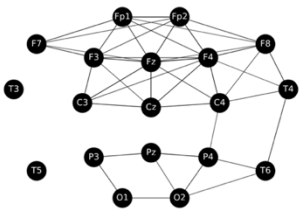

Figure ts02. Topographic arrow map for s02

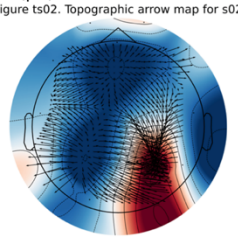

Figure gs02. Average connectivity for subject s02

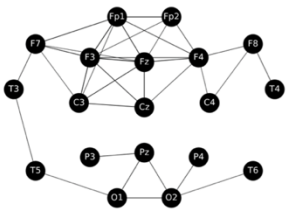

Figure ts03. Topographic arrow map for s03

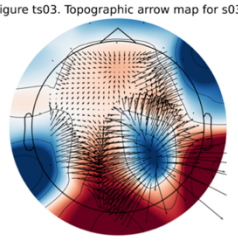

Figure gs03. Average connectivity for subject s03

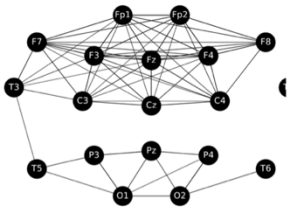

Figure ts04. Topographic arrow map for s04

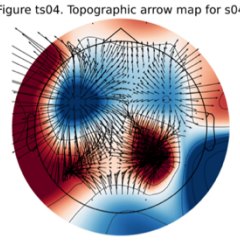

Figure gs04. Average connectivity for subject s04

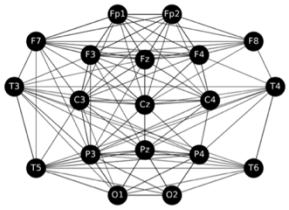

Figure ts05. Topographic arrow map for s05

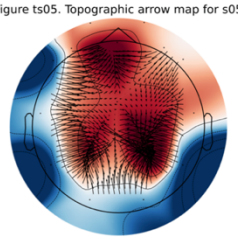

Figure gs05. Average connectivity for subject s05

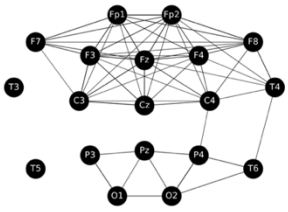

Figure ts06. Topographic arrow map for s06

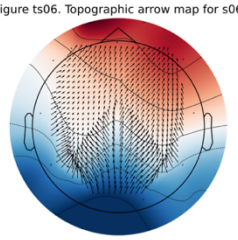

Figure gs06. Average connectivity for subject s06

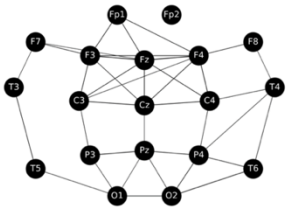

Figure ts07. Topographic arrow map for s07

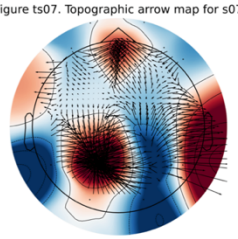

Figure gs07. Average connectivity for subject s07

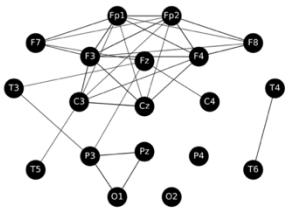

Figure ts08. Topographic arrow map for s08

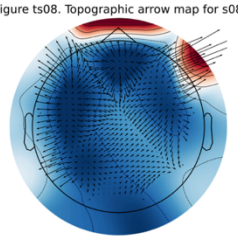

Figure gs08. Average connectivity for subject s08

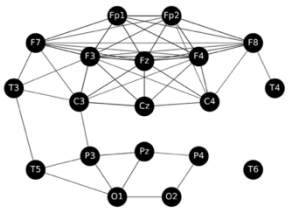

Figure ts09. Topographic arrow map for s09

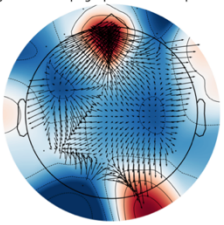

Figure gs09. Average connectivity for subject s09

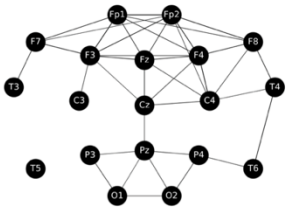

Figure ts10. Topographic arrow map for s10

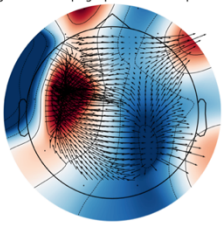

Figure gs10. Average connectivity for subject s10

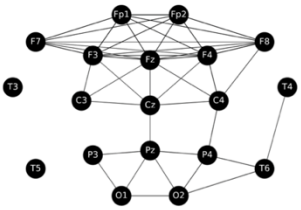

Figure ts11. Topographic arrow map for s11

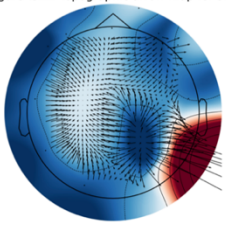

Figure gs11. Average connectivity for subject s11

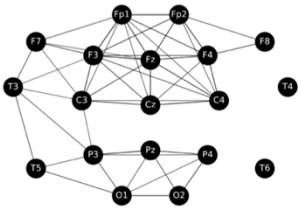

Figure ts12. Topographic arrow map for s12

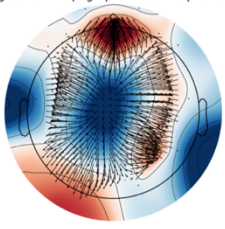

Figure gs12. Average connectivity for subject s12

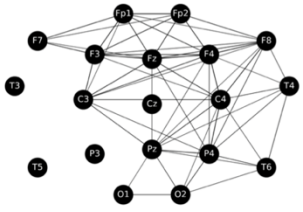

Figure ts13. Topographic arrow map for s13

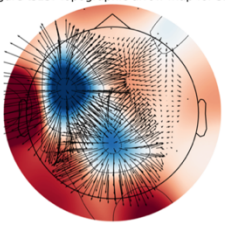

Figure gs13. Average connectivity for subject s13

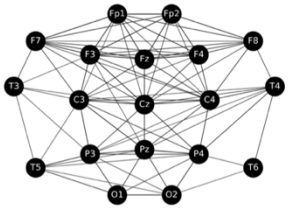

Figure ts14. Topographic arrow map for s14

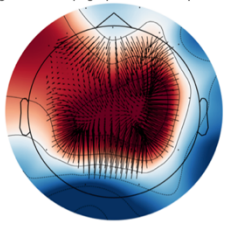

Figure gs14. Average connectivity for subject s14

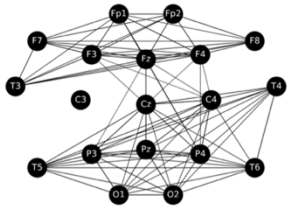

Control:

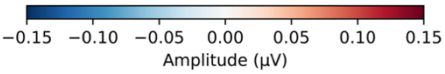

Figure th01. Topographic arrow map for h01

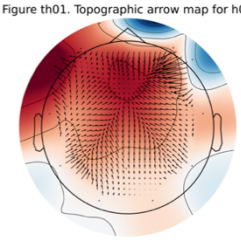

Figure gh01. Average connectivity for subject h01

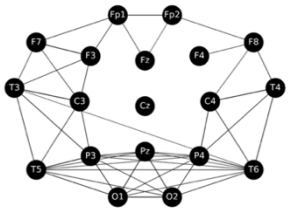

Figure th02. Topographic arrow map for h02

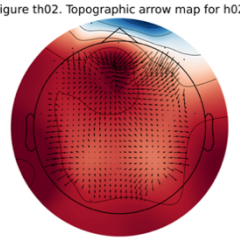

Figure gh02. Average connectivity for subject h02

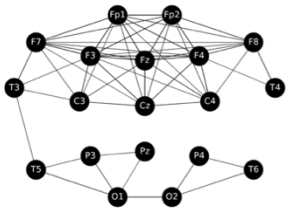

Figure th03. Topographic arrow map for h03

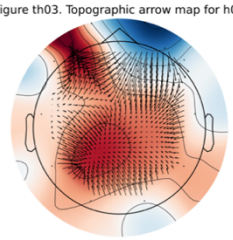

Figure gh03. Average connectivity for subject h03

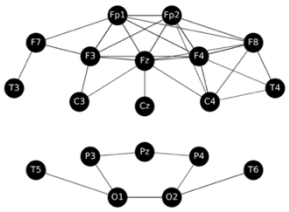

Figure th04. Topographic arrow map for h04

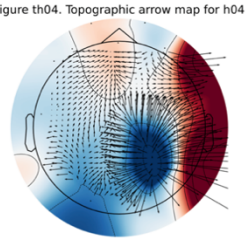

Figure gh04. Average connectivity for subject h04

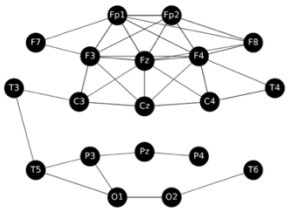

Figure th05. Topographic arrow map for h05

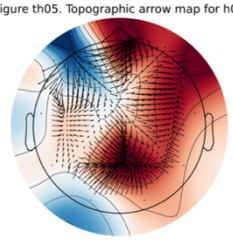

Figure gh05. Average connectivity for subject h05

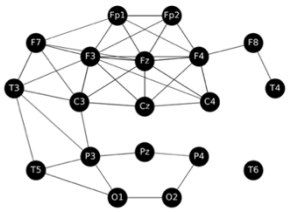

Figure th06. Topographic arrow map for h06

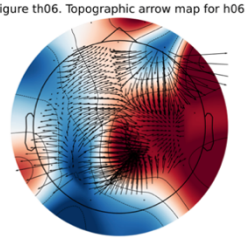

Figure gh06. Average connectivity for subject h06

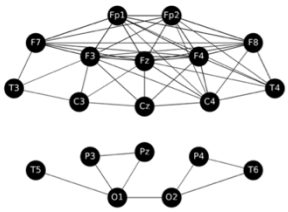

Figure th07. Topographic arrow map for h07

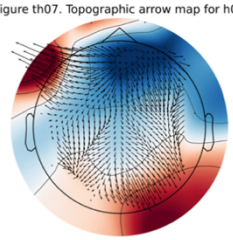

Figure gh07. Average connectivity for subject h07

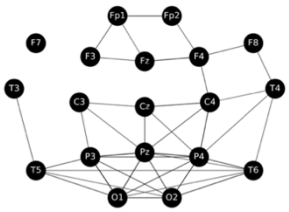

Figure th08. Topographic arrow map for h08

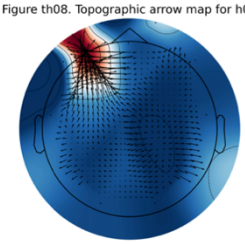

Figure gh08. Average connectivity for subject h08

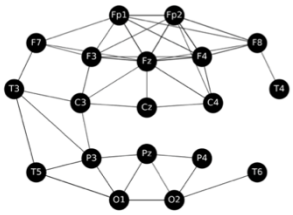

Figure th09. Topographic arrow map for h09

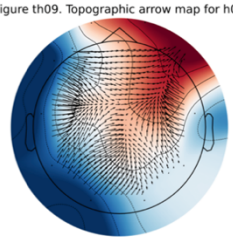

Figure gh09. Average connectivity for subject h09

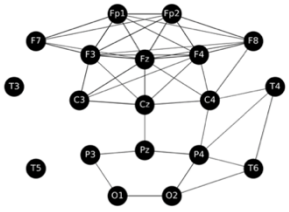

Figure th10. Topographic arrow map for h10

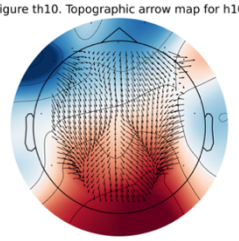

Figure gh10. Average connectivity for subject h10

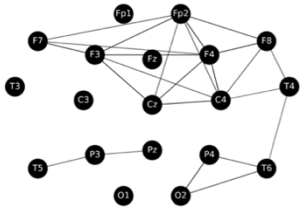

Figure th11. Topographic arrow map for h11

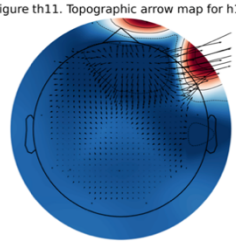

Figure gh11. Average connectivity for subject h11

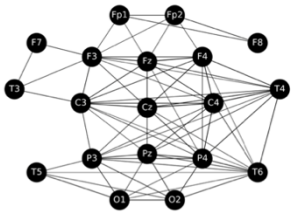

Figure th12. Topographic arrow map for h12

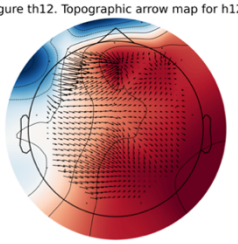

Figure gh12. Average connectivity for subject h12

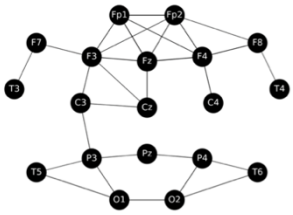

Figure th13. Topographic arrow map for h13

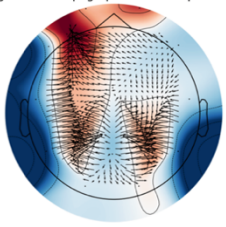

Figure gh13. Average connectivity for subject h13

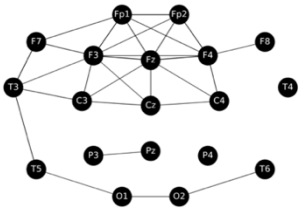

Figure th14. Topographic arrow map for h14

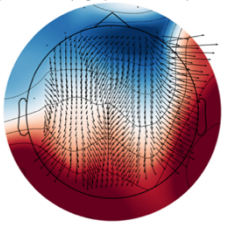

Figure gh14. Average connectivity for subject h14

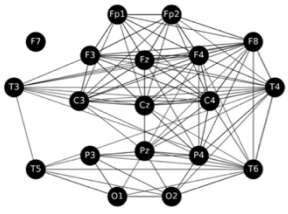

Feature extraction

The adjacency matrices were transformed using a discrete Fourier Transform (DFT) to extract spectral features. The real component of the transformed matrices was utilized, and eigenvalues were computed to capture the spectral properties of the brain connectivity networks.

Classification

A Random Forest classifier was used to differentiate between schizophrenia and control subjects. The model was encapsulated within a pipeline that included several steps. First, imputation was applied using SimpleImputer with a mean strategy to handle missing values. Next, feature scaling was performed using MinMaxScaler to ensure that all variables were on the same scale. Dimensionality reduction was then performed using Principal Component Analysis (PCA), retaining 95% of the variance. Finally, a RandomForestClassifier was employed with hyperparameters optimized via GridSearchCV.

The optimized hyperparameters included the number of estimators (n_estimators) set to 100, no restriction on maximum depth (max_depth), and the minimum number of samples required to split a node (min_samples_split) set to 10.

For cross-validation, a Stratified K-Fold Cross-Validation with 14 folds was used to ensure balanced class representation in each fold. The value of K was chosen as 14 to match the number of subjects, ensuring that each fold contained data from every subject, thus reducing subject-specific biases.

The cross-validation was applied to the entire pipeline, including feature extraction and hyperparameter tuning, to ensure that the evaluation metrics accurately reflected the model's performance on unseen data.

Evaluation metrics

Classification performance was evaluated using accuracy, precision, recall, F1-score, and confusion matrix. Cross-validation predictions were used to generate a comprehensive classification report, providing insights into the model's ability to identify both control and schizophrenia subjects correctly.

Results

The classification model achieved a Total Accuracy of 92.86%, with both control and schizophrenia classes exhibiting an Accuracy of 92.86% each. The Best Parameters identified through GridSearchCV were:

clf__n_estimators: 100
clf__max_depth: None
clf__min_samples_split: 10

The Classification Report is as follows:

	Precision	Recall	F1-Score	Support
Control	0.93	0.93	0.93	14
Schizophrenia	0.93	0.93	0.93	14
Accuracy			**0.93**	**28**
Macro Avg	0.93	0.93	0.93	28
Weighted Avg	0.93	0.93	0.93	28

The Confusion Matrix revealed:

[[13 1]
[1 13]]

The confusion matrix indicates that 13 of 14 control subjects were correctly classified, and one was misclassified. Similarly, 13 of 14 schizophrenia subjects were correctly classified, and one was misclassified.

Discussion

This study successfully demonstrated the efficacy of combining complex network analysis with DFT for diagnosing schizophrenia using EEG data. Achieving a 93% classification accuracy underscores the potential of this methodology in clinical settings. The rigorous validation process, which involves subject-by-subject verification and Stratified 14-fold Cross-Validation, ensures the reliability and robustness of the findings.

Compared to traditional EEG-based diagnostic tools, which often rely on time-domain or basic frequency-domain analyses, the integration of complex network analysis provides a more nuanced understanding of brain connectivity patterns. Unlike methods focusing solely on spectral features, our approach captures neural networks' structural and functional aspects, potentially uncovering biomarkers more specific to schizophrenia.

The attempted replication of a previously reported method, which claimed 100% accuracy, resulted in a considerably lower accuracy of 67%. This discrepancy highlights the importance of methodological transparency in clinical neuroscience applications. Our findings suggest that achieving high classification accuracy is contingent upon careful feature extraction, appropriate model selection, and robust cross-validation techniques.

The high precision and recall across both classes indicate that the model consistently distinguishes between schizophrenia and control subjects, minimizing both false positives and false negatives. This balance is crucial in clinical diagnostics to avoid misdiagnosis and ensure appropriate treatment interventions. The model's computational efficiency and scalability further enhance its suitability for real-time diagnostic applications in diverse clinical environments.

Conclusion

This study presents a novel and efficient approach for diagnosing schizophrenia using EEG data, complex network analysis, and Discrete Fourier Transform. The methodology achieved a high classification accuracy of 93%, demonstrating its potential as a reliable diagnostic tool. The approach's low computational cost, scalability, and flexibility make it well-suited for clinical applications, potentially facilitating early and accurate diagnosis of schizophrenia. Despite the promising results, further validation with larger and more diverse populations is essential to establish the method's generalizability and effectiveness across varied clinical settings. Integrating advanced computational techniques in psychiatric diagnostics represents a significant step forward in bridging the gap between neuroscience research and clinical practice.

Funding: The research in this paper was not supported by any external grant.

Conflicts of Interest: The author declares no conflict of interest. For a signed statement, contact the Editorial Office.

Quote this article as Vargas Cruz, Miguel Angel. 2025. "Paranoid Schizophrenia Diagnosis via Complex Network Analysis on EEG Data. "*Precis. Nanomed.*, 8(1) 1406–13. https://doi.org/10.33218/001c.128586.

References

[1] Olejarczyk, E., Jernajczyk, W. (2017). Graph-based analysis of brain connectivity in schizophrenia. PLOS ONE. DOI: 10.1371/journal.pone.0188629.

[2] Ide, M., Ohnishi, T., Toyoshima, M., Balan, S., Maekawa, M., Shimamoto-Mitsuyama, C., Iwayama, Y., Ohba, H., Watanabe, A., Ishii, T., Shibuya, N., Kimura, Y., Hisano, Y., Murata, Y., Hara, T., Morikawa, M., Hashimoto, K., Nozaki, Y., Toyota, T., Wada, Y., Tanaka, Y., Kato, T., Nishi, A., Fujisawa, S., Okano, H., Itokawa, M., Hirokawa, N., Kunii, Y., Kakita, A., Yabe, H., Iwamoto, K., Meno, K., Katagiri, T., Dean, B., Uchida, K., Kimura, H., Yoshikawa, T. (2019). Excess hydrogen

sulfide and polysulfides production underlies schizophrenia pathophysiology. Wiley. DOI: 10.15252/emmm.201910695.

[3] Hinkley, L., Vinogradov, S., Guggisberg, A., Fisher, M., Findlay, A., Nagarajan, S. (2011). Clinical symptoms and alpha band resting-state functional connectivity imaging in patients with schizophrenia: Implications for novel approaches to treatment. Elsevier. DOI: 10.1016/j.biopsych.2011.06.029.

[4] Narr, K., Thompson, P., Sharma, T., Moussai, J., Zoumalan, C., Rayman, J., Toga, A. (2001). Three-dimensional mapping of gyral shape and cortical surface asymmetries in schizophrenia: Gender effects. American Journal of Psychaitry. DOI: 10.1176/appi.ajp.158.2.244.

[5] Kim, K., Duc, N., Choi, M., Lee, B. (2021). EEG microstate features for schizophrenia classification. PLOS ONE. DOI: 10.1371/journal.pone.0251842.

[6] Li, M., Spaulding, W. (2016). The neuropsychopathology of schizophrenia: Molecules, brain systems, motivation, and cognition. Springer. DOI: 10.1007/978-3-319-30596-7.

[7] Bitanihirwe, B., Woo, T. (2013). Perineuronal nets and schizophrenia: The importance of neuronal coatings. Elsevier. DOI: 10.1016/j.neubiorev.2014.03.018.

[8] Woo, T. (2013). Neurobiology of schizophrenia onset. Springer. DOI: 10.1007/7854_2013_243.

[9] Bortolon, C., Raffard, S. (2015). Self-reported psychotic-like experiences in individuals with obsessive-compulsive disorder versus schizophrenia patients: Characteristics and moderation role of trait anxiety. Elsevier. DOI: j.comppsych.2014.10.011.

[10] Gabriel, A. (2010). Gabapentin adjunctive to risperidone or olanzapine in partially responsive schizophrenia: An open-label pilot study. Dove Medical Press. DOI: 10.2147/NDT.S13407.

[11] Aleman, A., Kahn, R., Selten, J. (2003). Sex differences in the risk of schizophrenia. American Medical Association. DOI: 10.1001/archpsyc.60.6.565.

[12] Schizophrenia Working Group of the Psychiatric Genomics Consortium (2014). Biological insights from 108 schizophrenia-associated genetic loci. Nature. DOI: 10.1038/nature13595.

[13] Gur, Raquel E., Gur, Ruben C., Kohler, C., Turetsky, B., Siegel, S., Kanes, S., Bilker, W., Brennan, A. (2004). A sexually dimorphic ratio of orbitofrontal to amygdala volume is altered in schizophrenia. Biological Psychiatry. DOI: 10.1016/j.biopsych.2003.10.009.

[14] Wolf, D., Ruparel, K., Elliott, M., Gur, Raquel E., Gur, Ruben C., Kohler, C., Bilker, W., Loughead, J., Lesko, K. (2007). Limbic activation associated with misidentification of fearful faces and flat affect in schizofrenia. American Medical Association. DOI: 10.1001/archpsyc.64.12.1356.

[15] Gur, Raquel E., Gur, Ruben C., Kohler, C., Siegel, S., Bilker, W., Lesko, K., Ragland, J. (2006). Flat affect in schizophrenia: Relation to emotion processing and neurocognitive measures. Oxford University Press. DOI: 10.1093/schbul/sbj041.

[16] Elliott, M., Gur, Raquel E., Gur, Ruben C., Kohler, C., Turetsky, B., Siegel, S., Kanes, S., Bilker, W., Loughead, J., Ragland, J., Snyder, W., Pratiwadi, R., Arnold, S. (2007). Visual attention circuitry in schizophrenia investigated with oddball event-related functional magnetic resonance imaging. American Journal of Psychaitry. DOI: 10.1176/ajp.2007.164.3.442.

[17] Goshvarpour, A., Goshvarpour, A. (2019). Schizophrenia diagnosis using innovative EEG feature-level fusion schemes. Springer. DOI: 10.1007/s13246-019-00839-1.

[18] Ciprian, C., Masychev, K., Ravan, M., Manimaran, A., Deshmukh, A. (2020). Diagnosing schizophrenia using effective connectivity of resting-state EEG data. MDPI. DOI: 10.3390/a14050139.

[19] Gomez, J. (2020). Characterization of neural activity using complex network theory: An application to the study of schizophrenia. Springer. DOI: 10.1007/978-3-030-49900-6.

[20] Mednick, S., Hollister, J. (1995). Neural development and schizophrenia: Theory and research. Springer. DOI: 10.1007/978-1-4615-1955-3.

[21] Kelly, B., Cotter, D., Denihan, C., Larkin, D., Murphy, P., Kinsella, A., Walsh, D., Waddington, J., Larkin, C., O'Callaghan, E., Lane, A. (2020). Neurological soft signs and dermatoglyphic anomalies in twins with schizophrenia. Cambridge University Press. DOI: 10.1016/j.eurpsy.2003.10.006.

[22] Migdalska, A., Mill, J. (2019). Epigenetic studies of schizophrenia: Current status and future directions. Elsevier. DOI: 10.1016/j.cobeha.2018.12.003.

[23] Besteher, B., Brambilla, P., Nenadić, I. (2020). Twin studies of brain structure and cognition in schizophrenia. Elsevier. DOI: 10.1016/j.neubiorev.2019.12.021.

[24] Okada, N., Fukunaga, M., Yamashita, F., Koshiyama, D., Yamamori, H., Ohi, K., Yasuda, Y., Fujimoto, M., Watanabe, Y., Yahata, N., Nemoto, K., Hibar, D. P., van Erp, T. G. M., Fujino, H., Isobe, M., Isomura, S., Natsubori, T., Narita, H., Hashimoto, N., Miyata, J., Koike, S., Takahashi, T., Yamasue, H., Matsuo, K., Onitsuka, T., Iidaka, T., Kawasaki, Y., Yoshimura, R., Watanabe, Y., Suzuki, M., Turner, J. A., Takeda, M., Thompson, P. M., Ozaki, N., Kasai, K., Hashimoto, R., COCORO, (2016). Abnormal asymmetries in subcortical brain volume in schizophrenia. Nature. DOI: 10.1038/mp.2015.209.

[25] Kahn, R., Haijma, S., Cahn, W., Koolschijn, P., Hulshoff, H. (2012). Brain volumes in schizophrenia: A meta-analysis in over 18000 subjects. Oxford University Press. DOI: 10.1093/schbul/sbs118.

[26] Kubicki, M., Shenton, M. (2020). Neuroimaging in schizophrenia. Springer. DOI: 10.1007/978-3-030-35206-6.

[27] Saarinen, A., Lyytikäinen, L. P., Hietala, J., Dobewall, H., Lavonius, V., Raitakari, O., Kähönen, M., Sormunen, E., Lehtimäki, T., Keltikangas-Järvinen, L. (2022). Magical thinking in individuals with high polygenic risk for schizophrenia but no non-affective psychoses—a general population study. Nature. DOI: 10.1038/s41380-022-01581-z.

[28] Wolfson, E. J., Fekete, T., Loewenstein, Y., Shriki, O. (2024). Multi-scale entropy assessment of magnetoencephalography signals in schizophrenia. Nature. DOI: 10.1038/s41598-024-64704-2.

[29] Andreasen, N., Flaum, M., Arndt, S., Miller, D., Nopoulos, P. (1995). A longitudinal study of symptom dimensions in schizophrenia: Prediction and patterns of change. American Medical Association. DOI: 10.1001/archpsyc.1995.03950170026004.

[30] Lajtha, A., Javitt, D., Kantrowitz, J. (2009). Handbook of neurochemistry and molecular neurobiology. Springer. DOI: 10.1007/978-0-387-30410-6.

[31] Vargas, M. (2024). References. https://www.miguelangelvargascruz.com/en/references